



Adsorption of crystal violet from aqueous solution by chemically modified phoenix tree leaves in batch mode

Xiaofeng Ren, Wei Xiao, Randi Zhang, Yu Shang, Runping Han*

*School of Chemistry and Molecular Engineering, Zhengzhou University, No. 100 of Kexue Road, Zhengzhou 450001, P.R. China
Tel. +86 371 67781757; Fax: +86 371 67781556; email: rphan67@zzu.edu.cn*

Received 11 September 2013; Accepted 27 September 2013

ABSTRACT

In this study, phoenix tree leaves were modified by NaOH solution, and modified tree leaves (MTL) were obtained. Then, MTL were characterized by Brunauer-Emmett-Teller, FTIR, and scanning electron microscopic and selected as adsorbent to remove crystal violet (CV) from aqueous solution in batch mode. FTIR analysis showed that hydroxyl and carbonyl groups on the surface of MTL. The experiments were carried out to discuss the influence of significant variables, such as the value of initial pH, adsorbent dosage, and salt concentration. The results demonstrated that the optimal pH was found to be nearly 8, and coexisted salt was disadvantage of CV adsorption. The equilibrium adsorption data were fitted using three adsorption isotherm models, the Langmuir, Freundlich and Redlich–Peterson (R–P) equations by nonlinear regressive method. The results showed that R–P model provided the best correlation, followed by the Langmuir model. Adsorption capacity (q_m) obtained from Langmuir equation was 510.3 mg/g at 293 K. The pseudo-first-order and pseudo-second-order equations were applied to the adsorption kinetic data, and the kinetic process was fitted better by the pseudo-second-order model. The thermodynamic parameters (ΔH° , ΔS° , and ΔG°) were evaluated at different temperatures. It was concluded that CV adsorption process be endothermic and spontaneous in nature. The spent leaves can be recovered by diluted hydrochloric acid solution and reused for three cycles with similar regeneration efficiency.

Keywords: Phoenix tree leaves; Adsorption; Crystal violet; Regeneration; Thermodynamic

1. Introduction

A considerable amount of synthetic dyes is consumed in textile, pharmaceutical, and paper industries worldwide. Nevertheless, it is considered that probably 12% of synthetic dyes are lost during producing and employing, and approximately 20% of the lost dyes entering the water resources ultimately through

trade effluent [1]. Environmental contamination and negative influence on public health have been caused by synthetic dyes owing to their grievous bioaccumulation in wildlife and agonizing ecotoxicological effects. Currently, the adsorption technique has been widely used to remove dye-containing effluents as a result of cheapness, high efficiency, and simplicity of design [2].

Crystal violet (CV) (CI 42555, MF $C_{25}H_{30}N_3Cl$, MW 408), belonging to the class of triarylmethane dyes (see Fig. 1), is generally used to dye silk and cotton to

*Corresponding author.

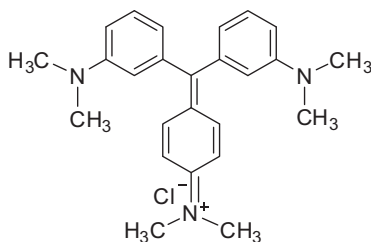


Fig. 1. The structure of crystal violet.

bluish violet color and to manufacture printing inks and paints. The dye is extremely toxic and carcinogenic. It can lead to moderate eye irritation and permanent injury to the conjunctiva and cornea. Inordinate exposure to CV may result in damage to digestive tract and skin, even causing kidney and respiratory failures [3]. Furthermore, CV is nonbiodegradable, scarcely metabolized by microorganism. As a result, it can exist chronically in various environments. Therefore, the removal of CV from solution is essential and important.

Nowadays, researchers have showed attention to low-cost adsorbents, such as agricultural by-products. The natural materials have enough potential in decoloration process owing to their wide applications, less expensive pretreatment step and environmental friendly [4,5]. Previously, several low-cost biomaterials have been reported to eliminate CV from effluent, such as grapefruit peel [3], rice bran [6], coir pith [7], wood apple [8], jackfruit leaf powder [9], and NaOH-modified rice husk [10].

The phoenix trees are extensively cultivated in China, such as in schools, parks and main roads of many cities. In autumn, a mass of natural phoenix tree leaves (NTL) fall to the ground and are almost completely discarded as waste. But the fallen leaves have already been reported to adsorb dyes from solution [11] as excellent adsorbent. The primary source of phoenix trees is lignin and cellulose. Hence, the leaves contain plentiful acidic groups, which are responsible for the adsorption of dyes. Therefore, the utilization of phoenix tree leaves as dyes adsorbents would not only solve the austere disposal problem but also represent a potential source of adsorbents, which will contribute to treat dyestuffs wastewater in a large degree.

To improve the performance of natural materials as the adsorbent, various modifications using different methods have been attempted. The most common chemical modifying agents are acids and bases. In this investigation, alkali treatment was researched to enhance adsorption properties. Treatment by sodium hydroxide (NaOH) solutions has a prominent effect on

molecular properties and morphological of cellulose, resulting to variation in pore structure, unit cell structure, accessibility, and crystallinity [12]. As a consequence, ion-exchange capacity and mechanical property of cellulose were improved. In addition, treatment with NaOH solution can remove natural waxes and fats from the surface of the cellulose. Thus, the reaction between dye ions and functional groups, such as hydroxyl group, can be carried out smoothly [13].

Consequently, this investigation was proceeded to explore the potential of utilizing NaOH-modified phoenix tree leaves (MTL) as environment-friendly and low-cost adsorbent to remove CV from solution. The influence of initial solution pH, adsorbent dose, and salt concentration has been researched. Adsorption isotherms, kinetics, and thermodynamic parameters were also estimated.

2. Materials and methods

2.1. Preparation of adsorbent

The phoenix tree leaves were collected from the new campus of Zhengzhou University in autumn and were washed roughly with distilled water to remove the mud, dust, and other impurities. The leaves were then dried at 333 K for 24 h in an oven. Subsequently, these dried leaves were crushed and screened to get specific geometrical sizes 20–40 mesh. The pretreated powder was stirred with sodium hydroxide (1%) in proportion of 1 g : 20 mL for 24 h at room temperature. The leaves were filtered and then washed using distilled water until the water was neutral. Definitely, the MTL were oven-dried to constant weight at 333 K. MTL were stored to remove CV.

2.2. Characterization of adsorbent

The surface areas of NTL and MTL were determined by nitrogen adsorption at 77 K using Brunauer–Emmett–Teller (BET) equation (Quantachrome NOVA 1000e, USA). Before the operation of N_2 adsorption, samples were outgassed at room temperature for 1.5 h. Micrographs of NTL and MTL were obtained using an SEM (JSM-6700F, Japan). Before observation, samples were coated with gold for several minutes to avoid charging.

FTIR spectra of samples were obtained using KBr pellets in the wave number range of $4,000\text{--}400\text{ cm}^{-1}$ (PE-1710 FTIR, USA). KBr wafers were prepared by mixing KBr crystals and a given weight of NTL and MTL. Then, the mixture was ground into powder and heated by FTIR lamp. Finally, under vacuum

conditions, the powder was pressed into KBr wafer and used for IR studies.

The zero point charge of MTL was estimated using the solid addition method. The determination experiment was conducted in a series of 50-mL shaking flasks containing 20 mL of NaCl (0.01 mol/L) with 0.01 g of adsorbent. The initial pH (pH_i) of salt solutions was controlled to 2–10 by adding either NaOH or HCl solution. The suspensions were then shaken until the equilibrium was reached after 12 h. The final pH (pH_f) of the solutions was determined.

2.3. Preparation of CV solution

CV used in this system was purchased from Yuanhang chemical reagent factory in Shanghai. The stock solutions of CV (1,000 mg/L) were prepared in double-distilled water. Experimental dye solutions of various concentrations were prepared by diluting the stock solution with appropriate volume of distilled water. All reagents and chemicals used for this study were of analytical grade.

2.4. Adsorption studies

Batch adsorption experiments were conducted in 50 mL-shaking flasks with 10 mL working solutions of known initial concentration. Certain amount of MTL was subjected to solutions. Then the flasks were agitated for 11 h at 303 K. The initial pH was adjusted using HCl and NaOH solutions. The effects of initial solution pH (2–12), amount of adsorbent (0.6–1.8 g/L), and salt concentration (0.01–0.10 mol/L) on adsorption quantity were performed, respectively.

For equilibrium studies, experiments were carried out in a series of conical flasks by contacting 0.01 g MTL with 10 mL CV solution of different initial concentrations, 100–1,000 mg/L. Then, these conical flasks were shaken for 11 h with temperatures 293, 303, and 313 K, respectively.

For kinetic studies, 0.01 g of MTL was subjected to the flasks and stirred with 10 mL dye solution of 100, 300, and 400 mg/L, respectively. For each initial dye concentration, a series of such conical flasks were then shaken at 293, 303 and 313 K for 11 h.

MTL were separated by filtration after adsorption. The residual concentration of CV was monitored using ultraviolet–visible spectrophotometer at λ_{max} of 620 nm.

2.5. Regeneration of spent adsorbent

When the adsorbent was exhausted by cationic dye (CV), aqueous solution of HCl (0.01 mol/L) was used

to desorb the dye, and MTL were regenerated. The conical flask containing 0.3 g CV-loaded MTL and 30 mL of HCl was shaken for 12 h at 303 K. After desorption, the MTL were centrifuged, and the dye concentration of supernatant solution was obtained with spectrophotometer analysis. Then, MTL were washed meticulously with distilled water and dried to constant weight. The dried MTL as regenerated adsorbent was employed to dislodge CV in the next cycle following the same method.

2.6. Error analysis

In order to determine the optimal model for certain adsorption system, experimental data were analyzed using the average relative error (ARE), combined with the determined coefficient (R^2). The values of ARE can be calculated using the following equation:

$$ARE = \frac{(\sum |(q_c - q_e)/q_e|)}{n} \quad (1)$$

where q_e and q_c are the experimental and calculated values, respectively; n is the number of the experimental points. The data were fitted by adsorption model using nonlinear regressive method (Origin 7.5 software).

3. Results and discussion

3.1. Characterization of adsorbent

3.1.1. Point of zero charge

In order to reasonably explain the adsorption mechanism, point of zero charge (pH_{zpc}) was investigated for MTL [14]. Then, plot ($\text{pH}_f - \text{pH}_i$) against pH_i was drawn, and the pH_{zpc} was the point when $\text{pH}_f - \text{pH}_i = 0$ [15] (figure not shown), which was evaluated to be 6.1.

3.1.2. BET analysis

The porous structure of the adsorbent is frequently probed by means of nitrogen adsorption at 77 K using BET equation.

The BET surface areas for NTL and MTL were approximately 2.08 and 1.74 m^2/g , respectively. The result definitely showed that alkali treatment inconsiderably affected the specific surface area of phoenix tree leaves.

3.1.3. SEM analysis

The SEM photographs revealed porosity and the external surface texture of the adsorbent.

The surface morphology of phoenix tree leaves was analyzed by SEM before and after alkali treatment (figure not shown). For NTL, surface micrograph showed porous and irregular surface with lots of uneven protrusions and cracks. After modification, distinct change was observed in structure of MTL. The smoother surface exhibited ordered structure, and regular caves and rifts distributed on the modified surface.

3.1.4. FTIR spectra

The FTIR spectral analysis was undertaken to get better insight into the important functional groups on the surface of leaves [16], which are responsible for the adsorption of CV ions. The FTIR of NTL and MTL before adsorption and after adsorption of CV were analyzed (figure not shown).

Several sharp and distant absorption peaks were illustrated on the FTIR spectrum before modification. The broad band near $3,416\text{ cm}^{-1}$ was assigned to the O–H stretching vibration in alcohols and phenols [17]. The peak at $2,925\text{ cm}^{-1}$ was due to asymmetrical stretching of aliphatic. Nevertheless, the wave number observed at $2,853\text{ cm}^{-1}$ denoted the presence of C–H symmetrical stretching. The characteristic peaks of the carbonyl group from carboxylic acids and ketones were verified at $1,733$ and $1,621\text{ cm}^{-1}$, respectively [18]. The peak at $1,375\text{ cm}^{-1}$ was attributed to C–H asymmetric bending vibration. The peak located at $1,243\text{ cm}^{-1}$ was due to stretch vibration of C–O in phenols of lignin. The adsorption peak at $1,100\text{--}1,300\text{ cm}^{-1}$ was indicative of C–O stretching vibrations in esters and alcohols.

After alkali treatment, the intensity of the band at $3,447$ and $1,635\text{ cm}^{-1}$ both decreased, indicating that sodium hydroxide may bind to hydroxyl and carbonyl groups during the process of modification.

Moreover, FTIR analysis was conducted after CV adsorption onto MTL. It was obvious that the characteristic peaks of O–H and C=O shift from $3,447$ and $1,635$ to $3,431$ and $1,624\text{ cm}^{-1}$, respectively. Generally, some chemical functional groups like carboxyl and hydroxyl demonstrated excellent coordination with dye ions. Therefore, these functional groups were confirmed to be primary adsorption sites for the adsorption of CV by MTL.

3.2. Adsorption studies

3.2.1. Effect of initial solution pH

The pH intensely influences the adsorption performance of the dye. Experiment was conducted at

predetermined conditions. The pH of the working solutions was adjusted by NaOH and HCl to a range of 2–12. The results were shown in Fig. 2.

As seen in Fig. 2, it was clear that the adsorption capacity was the lowest at the initial pH 2, and the value of q_e increased rapidly when the value of pH changed from 2.46 to 6.1. Further increase in adsorption was negligible between the pH of 6.1–11.05, revealing adsorption efficiency was improved obviously at higher pH. Similar behavior was found for the adsorption of CV onto Ananas pineapple leaf powder [19].

CV is almost completely ionized under any conditions and exists as the positively charged dye ions because of low value of pKa. At lower pH, the high concentration of hydrogen ions present in the solution would compete with CV^+ for insufficient active sites of the adsorbent. As a result, the removal of CV was impeded in acidic environment.

Additionally, the zero point of charge (pH_{zpc}) of the adsorbent plays a significant role in illustrating the influence of pH. The value of pH_{zpc} was about 6.1 obtained from the above-mentioned study. When pH is over 6.1, the surface charge of MTL was negative. But in contrast, there was positive in surface of MTL. At higher pH, the adsorptive capacity gradually reached the plateau values. This phenomenon was explained by the fact that the electrostatic attraction between the positively charged dye molecules and the negatively charged functional group (such as $-\text{COO}^-$) on the surface of MTL was facilitated in alkali condition.

Since maximum uptake was observed at pH 8.0, the value of 8 was selected as optimum pH for all the other experiments.

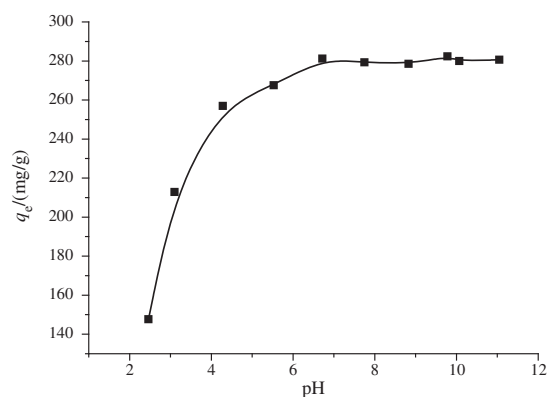


Fig. 2. Effect of pH on CV adsorption ($C_0 = 300\text{ mg/L}$).

3.2.2. Effect of adsorbent dose

In order to reach maximum capacity with possibly minimum amount, the quantity of the contacting sorbent [20] was studied qualitatively.

The graphical presentation was illustrated in Fig. 3. It was observed that the percent removal efficiency of CV increased from 73.8 to 95.9%, and the values of q_e reduced from 491.9 to 213.2 mg/g when the quantity of adsorbent changed from 0.6 to 1.8 g/L.

The increased percentage of dye removal was mainly attributed to much more active sites available for adsorption [21]. The similar result was reported by previous researcher [22]. On the other hand, the presence of redundantly unsaturated dye-binding sites on MTL led to lower removal of the dye. Furthermore, particulate interaction, such as aggregation may result in a longer diffusional path length [23], which aggravated the decline of adsorptive uptake of CV. Taking all these into consideration, leaf dose of 1 g/L was chosen for next studies.

3.2.3. Effect of salt concentration

Superfluous salts are currently used in the process of staining. Hence, effect of common salt concentration is significant in the study of adsorption. The influence of salt concentration (NaCl and CaCl₂) on adsorption of CV by MTL was depicted in Fig. 4.

It was apparent that both sodium chloride and calcium chloride co-existed in solution were adverse to the adsorption behavior. When the concentration of salt changes from 0.00 to 0.10 mol/L, the amount of CV adsorbed onto MTL (q_e) decreased from 374.9 to 278.4 and 140.2 mg/g for NaCl and CaCl₂, respectively. This trend was mainly responsible for the competition between cations from the salt and CV ions for

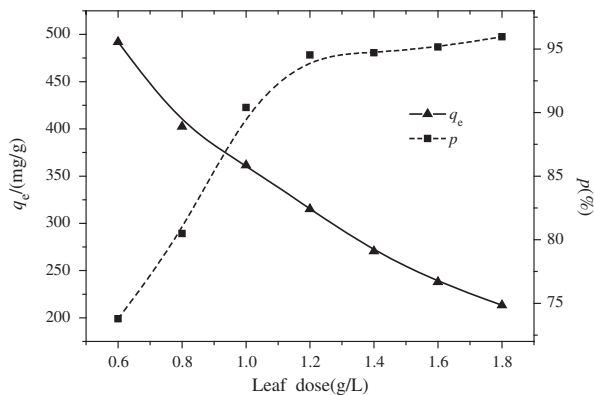


Fig. 3. The effect of MLT dose on the adsorption of CV on MTL ($C_0 = 400$ mg/L).

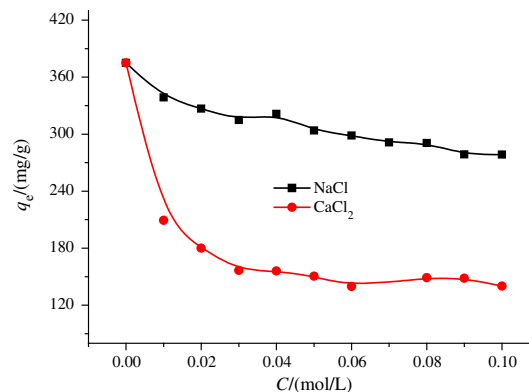


Fig. 4. The effect of salt concentration on the adsorption of CV on MTL ($C_0 = 400$ mg/L).

limited active sites during adsorption process. This implied that the mechanism of this reaction may be ion exchange. The other significant explanation was that the activity of adsorption sites reduced as the salt concentration increased. Thus, adsorption efficient of MTL declined markedly.

From Fig. 4, it was also found that the negative effect of Ca²⁺ on adsorption was more significant than Na⁺ when the other experimental conditions were same. This phenomenon was on account of bigger positive charge and larger ionic strength provided by Ca²⁺ than Na⁺.

3.2.4. Effect of equilibrium dye concentration

The influence of concentration of CV within dye solutions on adsorption capacity of MTL at 293, 303 and 313 K was illustrated in Fig. 5, respectively. It was noted that the values of q_e became larger with the increase of CV equilibrium concentration (C_e) at three different temperatures. This may be due to larger driving force caused by the concentration gradient at higher dye concentration [24]. On the other hand, much more CV ions were supplied for the same number of active sites, which can enhance the reaction of adsorption. As can be seen in Fig. 5, equilibrium uptake was 471.3 mg/g at 293 K. The value is much larger than previous observations [25,26].

Temperature is one of the important parameters in the study of dye adsorption and it is also a useful indicator to manifest the nature of reaction whether it is an endothermic or exothermic process. It was found that the adsorption uptake increased from 477.3 to 715.4 mg/g when temperature changed from 293 to 313 K. This trend fully suggested that the removal of CV on MTL was endothermic in nature. It was a result

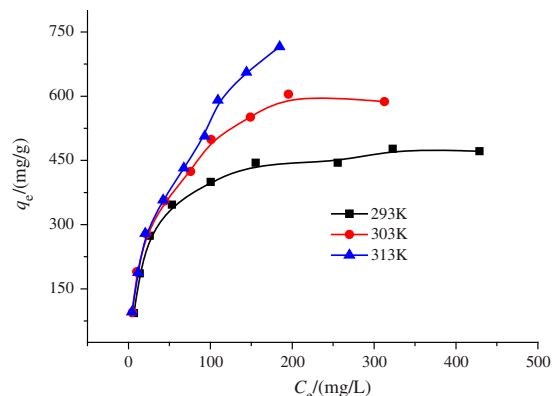


Fig. 5. Adsorption isotherms of CV-MTL system at three temperatures.

of stronger mobility of CV molecules and larger number of active sites at higher temperature [26].

3.2.5. Determination of adsorption isotherm parameters about CV/MTL system

The adsorption isotherm can describe the distribution of dye between solid phase and the solution at a certain temperature when the equilibrium was reached. The Langmuir, Freundlich and Redlich–Peterson (R–P) models were applied to fit the equilibrium data. Each isotherm model was expressed by relative certain constants which characterized the surface properties and indicated adsorption capacity of this material.

3.2.5.1. Langmuir isotherm. The Langmuir model proposes that monolayer sorption occurs on the solid surface with identical homogeneous sites [27]. It also suggests that no further adsorption takes place once the active sites are covered with dye molecules. The saturated monolayer isotherm is presented by the following equation:

$$q_e = \frac{q_m K_L C_e}{1 + K_L C_e} \quad (2)$$

where C_e is the concentration of dye at equilibrium in solution (mg/L); q_e is unit equilibrium adsorption capacity; q_m is the maximum dye uptake, giving the information about adsorption capacity for a complete monolayer (mg/g); and K_L is a constant denoted the energy of adsorption and affinity of the binding sites (L/mg).

3.2.5.2. Freundlich isotherm. Freundlich isotherm is an empirical model assuming the distribution of the

heat on the adsorbent surface is nonuniform, namely a heterogeneous adsorption [28]. The equation is stated as follows:

$$q_e = K_F C_e^{1/n} \quad (3)$$

where n and K_F [mg/g (L/mg) ^{n}] are both the Freundlich constants giving an indication of adsorption intensity and capacity, respectively.

3.2.5.3. R–P isotherm. The R–P model is empirical three-parameter isotherm combining the Langmuir and Freundlich isotherms [29]. It is based on the following equation:

$$q_e = \frac{AC_e}{1 + BC_e^g} \quad (4)$$

where g , A and B are the R–P parameters. g lies between 0 and 1.

The coefficients of determination (R^2) and isotherm parameters from nonlinear regressive method were all listed in Table 1. A comparison of nonlinear fitted curves from experimental data and three different isotherms at 293, 303 and 313 K was shown in Fig. 6.

The larger values of R^2 (≥ 0.970) and smaller ARE (≤ 0.122) indicated the applicability of the Langmuir isotherm for dye adsorption. q_m was an important Langmuir constant, representing the maximum capacity at equilibrium. Values of q_m increased, while

Table 1
Constants of adsorption isotherm models for CV adsorption onto MTL

T/K	293	303	313
<i>Langmuir</i>			
$K_L/(L/mg)$	0.0420	0.0304	0.0169
$q_m/(mg/g)$	501.3	662.2	902.3
R^2	0.994	0.981	0.970
ARE	0.0364	0.0612	0.122
<i>Freundlich</i>			
K_F	107.9	95.9	58.2
$1/n$	0.259	0.337	0.483
R^2	0.890	0.939	0.993
ARE	0.177	0.141	0.491
<i>Redlich–Peterson</i>			
A	20.2	25.6	85.2
B	0.0367	0.064	1.06
g	1.02	0.911	0.571
R^2	0.994	0.985	0.993
ARE	0.0352	0.0498	0.0416

Notes: R^2 : determined coefficient; ARE : average relative error.

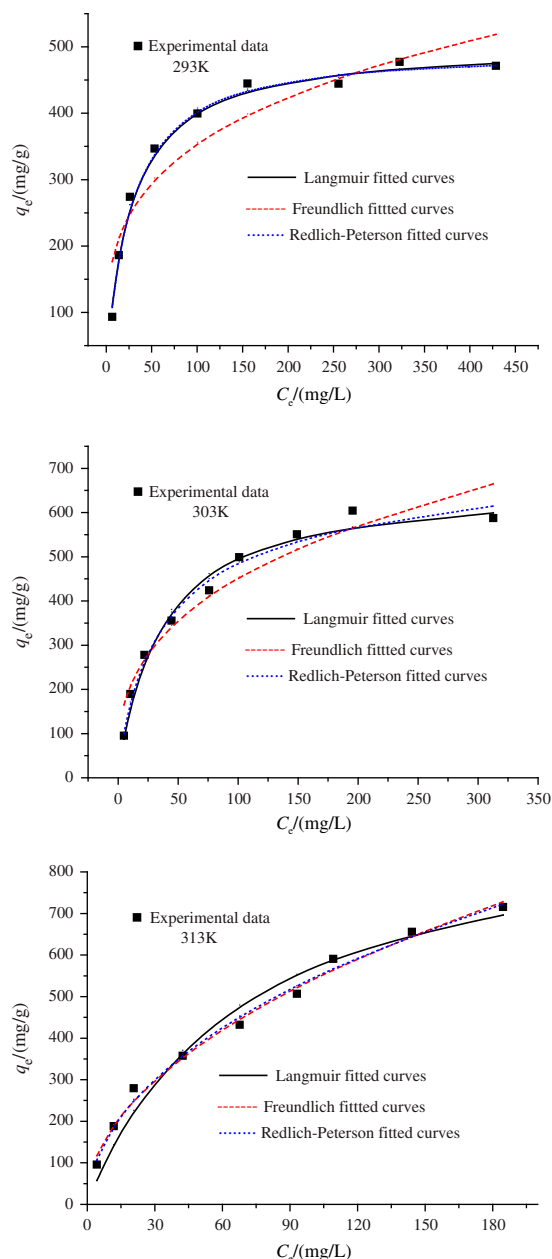


Fig. 6. Comparison of experimental points and the nonlinear fitted curves from three isotherm models.

the values of K_L decreased with the rise of temperature.

The Freundlich model did not provide any information about the saturation adsorption capacity as well as Langmuir model with lower R^2 (0.890) and higher error. The parameters of K_F and $1/n$ exhibited intense change at higher temperature. The values of $1/n$ ($0.1 < 1/n < 1$) indicated favorable adsorption of CV at experimental conditions.

The equilibrium data were fitted best to the R–P model with the highest R^2 and lowest ARE . It was found that the values of A and B became larger with the rise in temperature. What's more, the parameter g was near to 1 at 293 and 303 K, suggesting that the model was approaching the Langmuir isotherm.

Moreover, it was observed from Fig. 6 that the fitted curves from the R–P isotherm were most near to the experimental data at experimental conditions. Hence, the R–P model was best to describe adsorption behavior at equilibrium.

From Table 1, the maximum adsorption capacity (q_m) of MTL for CV removal was up to 510.3 mg/g at 293 K. There were many studies of CV adsorption by low-cost materials derived from plants, and values of adsorption capacity toward CV were presented, such as grapefruit peel 249.7 mg/g [3], rice bran 42.3 mg/g [6], coir pith 2.56 mg/g [7], wood apple 19.8 mg/g [8], Jackfruit leaf powder 43.4 mg/g [9], NaOH-modified rice husk 44.9 mg/g [10], tomato plant root (94.3 mg/g [30], neem sawdust 3.8 mg/g [31], Pinus bark powder 32.8 mg/g [32], value of q_m of CV adsorption onto MTL is highest. So MTL was competent as adsorbent to remove CV from solution.

3.2.6. Effect of contact time and analysis of kinetic constants

The results of adsorption quantity per MTL (q_t) at different contact time (t) are shown in Fig. 7. From Fig. 7, it was shown that the adsorption of CV onto MTL increased with increasing the contact time at different conditions. Kinetics of adsorption of CV consisted of two phases: an initial rapid phase where adsorption was fast and contributed significant to equilibrium uptake and a slower second phase whose contribution to the total CV adsorption was relatively small. It was also seen that equilibrium time occurred relatively earlier in the solution containing lower CV concentrations. The necessary time to reach equilibrium was variable according to the initial concentration. So the adsorptive quantity of MTL at equilibrium increased with the increase in initial CV concentration.

In order to analyze the sorption kinetics of CV, both the pseudo-first-order and the pseudo-second-order models were applied to the experimental data in this study.

3.2.6.1. Pseudo-first-order kinetic model. The pseudo-first-order kinetic model was presented as follows [33]:

$$q_t = q_e(1 - e^{-k_1 t}) \quad (5)$$

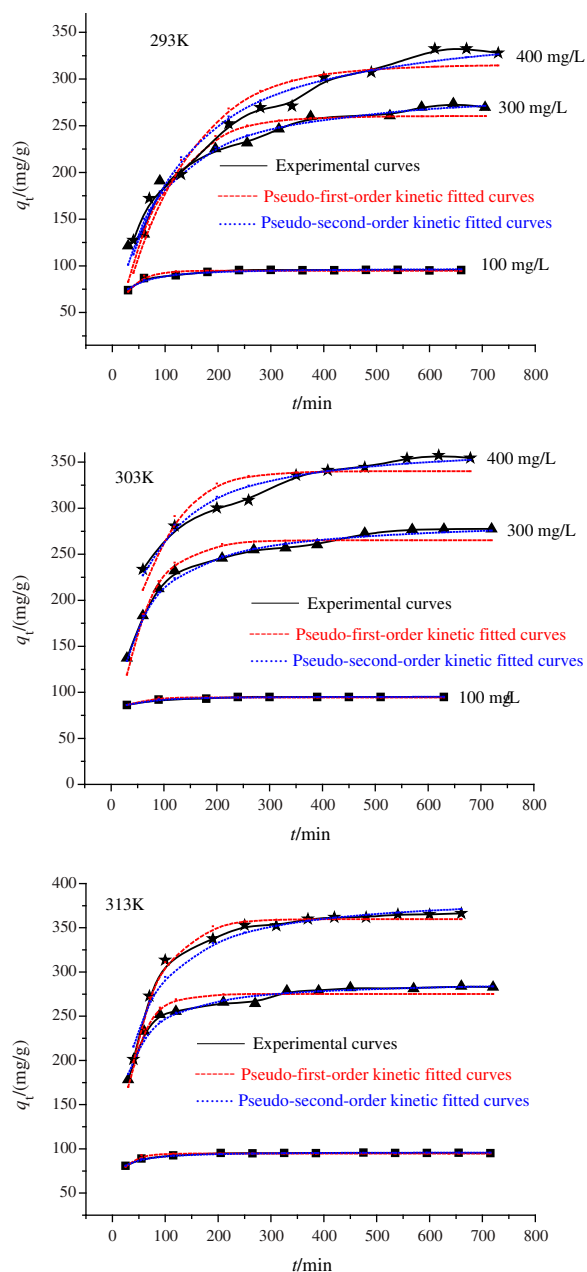


Fig. 7. The experimental points and nonlinear fitted curves with kinetic models.

where q_e and q_t (mg/g) were the amounts of CV adsorbed on adsorbent at equilibrium and at any time t , respectively. And k_1 was the rate constant of pseudo-first-order reaction (min^{-1}).

3.2.6.2. Pseudo-second-order kinetic model. The pseudo-second-order equation can be expressed as follows [34]:

$$q_t = \frac{k_2 q_e^2 t}{1 + k_2 q_e t} \quad (6)$$

where k_2 was rate constant of pseudo-second-order adsorption (g/mg min).

The values of k_1 , k_2 , and q_e can be calculated using nonlinear regressive analysis. The relative parameters and determined coefficient (R^2) were all listed in Table 2. Moreover, the comparison between fitted curves and experimental data were also illustrated in Fig. 7.

Generally, the best-fit model can be chosen according to the determined coefficient and error analysis. From Table 2, the values of R^2 from the pseudo-second-order kinetic model ranged from 0.965 to 0.992, which was higher than those from the pseudo-first-order kinetics at three different temperatures. While the higher values of ARE for the pseudo-first-order kinetic model confirmed the nonapplicability of this model. Thus, it was indicated that the pseudo-second-order kinetic model was better to fit to the experimental data, while pseudo-first-order kinetic model was available to fit. This supports the assumption [35] that the rate-limiting step of CV onto MTL may be chemisorption.

It was also clear in Table 2 that adsorption uptake increased slightly with temperature rise. This suggested that the adsorption process is endothermic in nature and a higher temperature was in favor of CV removal.

The predicted curves from the pseudo-first-order and pseudo-second-order models were compared with the corresponding experimental results (Fig. 7). As depicted in Fig. 7, the experimental data were not very close to nonlinear fitted curves from the pseudo-first-order model. Hence, this model cannot predict the adsorption process because of large discrepancies. On the contrary, a good agreement was found between the predicted and experimental curves from the pseudo-second-order model. So, it was reasonably to refer that the pseudo-second-order model was suitable to predict the experimental data.

3.2.7. Calculation of thermodynamic parameters

The influence of temperature on the adsorption of CV with MTL can be explained thermodynamically by determining parameters, such as change in enthalpy (ΔH°), entropy (ΔS°), and free energy (ΔG°). The apparent equilibrium constant (K_c) was evaluated using the following equation [36,37]:

$$K_c = \frac{c_{ad,e}}{C_e} \quad (7)$$

where $c_{ad,e}$ is equilibrium concentration of CV on the adsorbent (mg/L).

Table 2
Kinetic parameters for adsorption of CV on MTL

T/K C ₀ /(mg/L)	293 K			303 K			313 K		
	100	300	400	100	300	400	100	300	400
Pseudo-first-order model									
$k_1 \times 10^{-2}$ (1/min)	4.84	1.28	0.87	8.14	1.99	1.62	7.40	3.21	2.02
q_e /(mg/g)	94.7	260.4	315.0	94.5	265.3	340.2	94.7	275.2	359.8
R^2	0.922	0.919	0.906	0.883	0.934	0.811	0.873	0.926	0.986
ARE	0.0151	0.0667	0.0843	0.0079	0.037	0.046	0.012	0.0286	0.0135
Pseudo-second-order model									
$k_2 \times 10^{-3}$ (g/mg min)	1.14	0.06	0.03	3.17	0.1	0.07	2.18	0.20	0.08
q_e /(mg/g)	97.7	293.3	367.2	95.7	288.9	372.5	96.5	290.6	389.2
R^2	0.976	0.973	0.970	0.983	0.992	0.965	0.990	0.975	0.974
ARE	0.009	0.0423	0.0453	0.0027	0.0146	0.0169	0.0032	0.0148	0.02

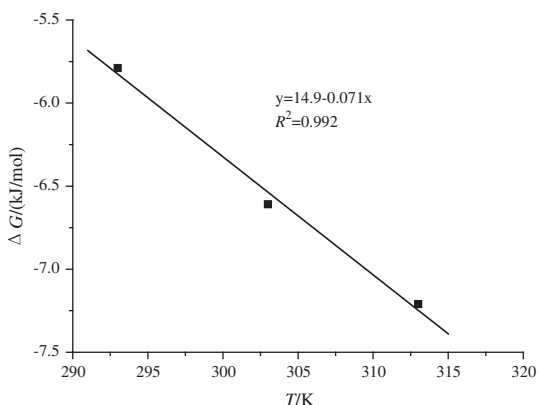


Fig. 8. Plot of Gibbs free energy change versus temperature for adsorption of CV by MTL.

$$\Delta G^0 = -RT \ln K_c \quad (8)$$

$$\Delta G^0 = \Delta H^0 - T\Delta S^0 \quad (9)$$

ΔG^0 was computed by means of the value of K_c . The plot of ΔG^0 versus T was a straight line (Fig. 8) and the values of ΔS^0 and ΔH^0 were calculated from the slope and intercept of this plot, respectively.

The values of thermodynamic parameters for the adsorption of CV on MTL were listed in Table 3.

Table 3
Thermodynamic parameters of CV adsorption on MTL

T/K	293	303	313
ΔG^0 (kJ/mol)	-5.79	-6.61	-7.21
ΔH^0 (kJ/mol)		14.9	
ΔS^0 (kJ/mol K)		0.071	

The standard entropy and enthalpy changes of adsorption were found to be 0.071 kJ/mol K and 14.9 kJ/mol in Table 3, respectively. The CV adsorption was temperature-dependent and endothermic in nature throughout the process, giving a positive value of ΔH^0 . So the adsorption of CV onto MTL may be a chemical adsorption process. Moreover, the positive value of entropy change suggested the increased randomness at the solid/solution interface and some structural changes in the adsorbate and adsorbent. A positive value of (ΔS^0) also provide good affinity toward dye molecules [38,39]. In addition, small value of ΔS^0 gave the information of slight change on entropy. The negative values of free energy demonstrated the spontaneous and feasibility of the adsorption process. The decreased ΔG^0 with increasing temperature referred the feasibility of process at higher temperature.

3.2.8. Desorption of CV from MTL

Regeneration of exhausted adsorbent is of great concern due to environmental and economic motivations [40–42]. In this study, the adsorption/desorption cycles of CV were carried out three times repeatedly to estimate the reusability of MTL by soaking in hydrochloric solution (0.01 mol/L).

Table 4
The adsorptive quantity and regeneration rate of regenerated MTL

Cycle	q_e (mg/g)	Regeneration rate (%)
1	142.2	57.8
2	134.2	53.8
3	112.7	42.7

The adsorption performance of regenerated MTL was presented in Table 4. It was clear that the loss of adsorption capacity was insignificant in successive cycles of adsorption/desorption. The decrease of regeneration rate was slightly obvious during the third cycle.

Overall, successful recovery and high adsorptive uptake demonstrated that treatment of hydrochloric solutions was effective for reuse in dye-loaded MTL.

4. Conclusion

The prepared MTL was characterized by FITR, SEM, BET, pH_{zpc} and it was used as adsorbent to remove CV from solution in batch mode. Optimal pH was 8, and common salt coexisted in solution is not favor of adsorption. The adsorption of CV was depended on initial pH, adsorbent dosage and salt concentration. The Langmuir and R-P isotherms adequately described the behavior of equilibrium adsorption, and the maximum adsorption capacity (q_m) was up to 510.3 mg/g at 293 K. The kinetic studies showed this adsorption complied well with the pseudo-second-order model. Thermodynamic computation indicated endothermic and spontaneous process. CV-loaded leaves can be efficiently reused by soaking in diluted hydrochloric acid solution. The results of experiment suggested that MTL was suitable as adsorbent material to eliminate CV from wastewater.

Acknowledgment

This study was supported by the National Natural Science Foundation of China for undergraduate cultivation in basic science (J1210060).

References

- [1] A. Mittal, R. Jain, J. Mittal, M. Shrivastava, Adsorptive removal of hazardous dye quinoline yellow from wastewater using coconut-husk as potential adsorbent, *Fresenius Environ. Bull.* 19 (2010) 1–9.
- [2] M.A.M. Salleh, D.K. Mahmoud, W.A.W. A. Karim, A. Idris, Cationic and anionic dye adsorption by agricultural solid wastes: A comprehensive review, *Desalination* 280 (2011) 1–13.
- [3] A. Saeed, M. Sharif, M. Iqbal, Application potential of grapefruit peel as dye sorbent: Kinetics, equilibrium and mechanism of crystal violet adsorption, *J. Hazard. Mater.* 179 (2010) 564–572.
- [4] J.Y. Song, W.H. Zou, Y.Y. Bian, F.Y. Su, R.P. Han, Adsorption characteristics of methylene blue by peanut husk in batch and column mode, *Desalination* 265 (2011) 119–125.
- [5] A. Mittal, D. Jhare, J. Mittal, Adsorption of hazardous dye Eosin Yellow from aqueous solution onto waste material De-oiled Soya: Isotherm, kinetics and bulk removal, *J. Mol. Liq.* 179 (2013) 133–140.
- [6] X.S. Wang, X. Liu, L. Wen, Y. Zhou, Z. Li, Comparison of basic dye crystal violet from aqueous solution by low-cost biosorbents, *Sep. Sci. Technol.* 43 (2008) 3712–3731.
- [7] C. Namasivayam, M.D. Kumar, K. Selvi, R.A. Begum, T. Vanathi, R.T. Yamuna, “Waste” coir pith—a potential biomass for the treatment of dye in wastewaters, *Bio-mass Bioenergy* 6 (2001) 477–483.
- [8] R. Kumar, R. Ahmad, Biosorption of hazardous crystal violet dye from aqueous solution onto treated ginger waste (TGW), *Desalination* 265 (2011) 112–118.
- [9] P.D. Saha, S. Chakraborty, S. Chowdhury, Batch and continuous (fixed-bed column) biosorption of crystal violet by *Artocarpus heterophyllus* (jackfruit) leaf powder, *Colloid Surf., B* 92 (2012) 262–270.
- [10] S. Chakraborty, S. Chowdhury, P.D. Saha, Adsorption of crystal violet from aqueous solution onto NaOH-modified rice husk, *Carbohydr. Polym.* 86 (2011) 1533–1541.
- [11] R.P. Han, W.H. Zou, W.H. Yu, S.J. Cheng, Y.F. Wang, J. Shi, Biosorption of methylene blue from aqueous solution by fallen phoenix tree’s leaves, *J. Hazard. Mater.* 141 (2007) 156–162.
- [12] J. Siroky, R.S. Blackburn, T. Bechtold, J. Taylor, P. White, Alkali treatment of cellulose α fibres and effect on dye sorption, *Carbohydr. Polym.* 84 (2011) 299–307.
- [13] B.S. Naazi, S. Karloss, J.V. Tesha, C.W. Nyahumwa, Chemical and physical modification of rice husks for use as composite panels, *Compos Part A.* 38 (2007) 925–935.
- [14] A.A. Poghosian, Determination of the pH pzc of insulators surface from capacitance-voltage characteristics of MIS and EIS structures, *Sens. Actuator B.* 44 (1997) 551–553.
- [15] B.H. Hameed, I.A.W. Tan, A.L. Ahmad, Adsorption isotherm, kinetic modeling and mechanism of 2,4,6-trichlorophenol on coconut husk-based activated carbon, *Chem. Eng. J.* 144 (2008) 235–244.
- [16] A. Tabak, E. Eren, B. Afsin, B. Caglar, Determination of adsorptive properties of a Turkish sepiolite for removal of reactive blue 15 anionic dye from aqueous solutions, *J. Hazard. Mater.* 161 (2009) 1087–1094.
- [17] Y. Safa, H.N. Bhatti, Kinetic and thermodynamic modeling for the removal of Direct Red-31 and Direct Orange-26 dyes from aqueous solutions by rice husk, *Desalination* 272 (2011) 313–322.
- [18] S. Noreen, H.N. Bhatti, S. Nausheen, S. Sadaf, M. Ashfaq, Batch and fixed bed adsorption study for the removal of Drimarine Black CL-B dye from aqueous solution using a lignocellulosic waste: A cost affective adsorbent, *Ind. Crop Prod.* 50 (2013) 568–579.
- [19] S. Chakraborty, S. Chowdhury, P.D. Saha, Insight into biosorption equilibrium, kinetics and thermodynamics of crystal violet onto *Ananas comosus* (pineapple) leaf powder, *Appl. Water Sci.* 2 (2012) 135–141.
- [20] S.I. Zafar, M. Bisma, A. Saeed, M. Iqbal, FTIR spectrophotometry, kinetics and adsorption isotherms modeling, and SEM-EDX analysis for describing mechanism of biosorption of the cationic basic dye methylene blue by a new biosorbent (sawdust of silver fir; *Abies pindrow*), *Fresenius Environ. Bull.* 17 (2008) 2109–2121.

- [21] A.E. Ofomaja, Sorptive removal of Methylene blue from aqueous solution using palm kernel fibre: Effect of fibre dose, *Biochem. Eng. J.* 40 (2008) 8–18.
- [22] A. Saeed, M. Sharif, M. Iqbal, Application potential of grapefruit peel as dye sorbent: Kinetics, equilibrium and mechanism of crystal violet adsorption, *J. Hazard. Mater.* 179 (2010) 564–572.
- [23] O. Aksakal, H. Uzun, Equilibrium, kinetic and thermodynamic studies of the biosorption of textile dye (Reactive Red 195) onto *Pinus Sylvestris L.*, *J. Hazard. Mater.* 181 (2010) 666–672.
- [24] Y. Bulut, H. Aydin, A kinetics and thermodynamics study of methylene blue adsorption on wheat shells, *Desalination* 194 (2006) 259–267.
- [25] F. Atmani, A. Bensmaili, N.Y. Mezenner, Synthetic textile effluent removal by skin almonds waste, *J. Environ. Sci. Technol.* 2 (2009) 153–169.
- [26] S. Senthilkumar, P. Kalaamani, C.V. Subbaram, Liquid phase adsorption of crystal violet onto activated carbons derived from male flowers of coconut tree, *J. Hazard. Mater.* 136 (2006) 800–808.
- [27] I. Langmuir, Adsorption of gases on plain surfaces of glass mica platinum, *J. Am. Chem. Soc.* 40 (1918) 1361–1403.
- [28] H.M.F. Freundlich, Over the adsorption in solution, *J. Phys. Chem.* 57 (1906) 385–471.
- [29] O. Redlich, D.L. Peterson, A useful adsorption isotherm, *J. Phys. Chem.* 63 (1959) 1024–1026.
- [30] C. Kannan, N. Buvanewari, T. Palvannan, Removal of plant poisoning dyes by adsorption on tomato plant root and green carbon from aqueous solution and its recovery, *Desalination* 249 (2009) 1132–1138.
- [31] S.D. Khattri, M.K. Singh, Colour removal from synthetic dye wastewater using a bioadsorbent, *Water Air Soil Pollut.* 120 (2000) 283–294.
- [32] R. Ahmad, Studies on adsorption of crystal violet dye from aqueous solution onto coniferous pinus bark powder (CPBP), *J. Hazard. Mater.* 171 (2009) 767–773.
- [33] Y.S. Ho, J.C.Y. Ng, G. McKay, Kinetics of pollutant sorption by biosorbents: Review, *Sep. Purif. Method.* 29 (2000) 189–232.
- [34] Y.S. Ho, G. McKay, Pseudo-second order model for sorption process, *Process. Biochem.* 34 (1999) 451–465.
- [35] F.C. Wu, R.L. Tseng, R.S. Juang, Enhanced abilities of highly swollen chitosan beads for color removal and tyrosinase immobilization, *J. Hazard. Mater.* 81 (2001) 167–177.
- [36] Z. Aksu, Determination of the equilibrium, kinetic and thermodynamic parameters of the batch biosorption of lead(II) ions onto *Chlorella vulgaris*, *Process Biochem.* 38 (2002) 89–99.
- [37] C. Namasivayam, K. Ranganathan, Waste Fe(III)/Cr(III) hydroxide as adsorbent for the removal of Cr(VI) from aqueous solution and chromium plating industry wastewater, *Environ. Pollut.* 82 (1993) 255–261.
- [38] J. Mittal, V. Thakur, A. Mittal, Batch removal of hazardous azo dye Bismark Brown R using waste material hen feather, *Ecol. Eng.* 60 (2013) 249–253.
- [39] A. Mittal, V. Thakur, V. Gajbe, Adsorptive removal of toxic azo dye Amido Black 10B by hen feather, *Environ. Sci. Pollut. Res.* 20 (2013) 260–269.
- [40] V.K. Gupta, A. Mittal, D. Jhare, J. Mittal, Batch and bulk removal of hazardous colouring agent Rose Bengal by adsorption techniques using bottom ash as adsorbent, *RSC Adv.* 2 (2012) 8381–8389.
- [41] Y.Y. Su, Y.B. Jiao, C.C. Dou, R.P. Han, Biosorption of methyl orange from aqueous solutions using cationic surfactant-modified wheat straw in batch mode, *Desalin. Water Treat.* (2013), doi:10.080/19443994.2013.811121.
- [42] M. Asgher, H.N. Bhatti, Mechanistic and kinetic evaluation of biosorption of reactive azo dyes by free, immobilized and chemically treated *Citrus sinensis* waste biomass, *Ecol. Eng.* 36 (2010) 1660–1665.